Journal of Science and Technology in Civil Engineering, HUCE, 2025, 19 (2): 133–144

ANALYSIS OF STRESS CONCENTRATION FACTOR OF CORRODED STEEL MEMBER UNDER FATIGUE LOAD VERSUS TIME

Dao Duy Kien[a,*]

[a]*Faculty of Civil Engineering, Ho Chi Minh City University of Technology and Education, 01 Vo Van Ngan street, Thu Duc district, Ho Chi Minh city, Vietnam*

Article history:
Received 22/10/2024, Revised 23/4/2025, Accepted 08/5/2025

Abstract

This study focuses on analyzing the fatigue behavior of corroded steel structures. Accordingly, the accelerated corrosion experiments on steel structure working with concrete were conducted in the laboratory. Due to the increasing number of corrosion cycles to analyze the corrosion change process over time. The obtained corrosion specimens were taken out to conduct the fatigue behavior. The crack formation and propagation leading to fatigue damage combined with corrosion is very complex. This study proposed a method to determine the stress concentration factor K_t by the finite element method. Based on that, the optimal size, element mesh, and number of layers on the FEM model were also specifically presented. The confidence curve was proposed to design the fatigue life (S-N) of corroded steel plate in contact with concrete in terms of effective thickness. The results from this study will add useful knowledge to the design and maintenance of steel structures in practice.

Keywords: artificially; corroded steel; fatigue behavior; stress concentration factor; crack.

https://doi.org/10.31814/stce.huce2025-19(2)-10

1. Introduction

Corrosion creates the formation of many holes on the surface of steel structures, including uniform, pitting, crevice, galvanic, erosion, intergranular, and stress corrosion [1]. The distribution of corrosion on the surface of steel structures is random and difficult to predict accurately. However, the localized corrosion will concentrate at the joint or the boundary of the steel structure and other structures [2–5].

According to the serious consequences that corrosion has caused, it is realized that corrosion has completely changed the volume of steel structures, and chemical composition, these factors are considered direct risks leading to the degradation in bearing capacity as well as the life span of the steel structure which can lead to the sudden destruction [6–8]. The process of destroying metal structures due to corrosion takes place all over the world. Studies by the National Association of Corrosion Engineers (NACE) estimate that the global cost of corrosion could be as high as $2.5 trillion per year, or about 3-4% of global GDP. Corrosion also affects all aspects of social life, safety and health, and environmental pollution etc [9]. Corrosion becomes an economic barrier because of the need to continuously protect steel structures from corrosion.

Research on corrosion of steel structures is carried out with many environments, from atmospheric exposure corrosion, natural corrosion building that have reached the end of their life then corroded members such as beam, column are cut out for research, to accelerated corrosion method and artificial corrosion methods using mechanics... All experimental methods, simulation, finite element analysis

*Corresponding author. *E-mail address:* kiendd@hcmute.edu.vn (Kien, D. D.)

are included in the corrosion research. However, for steel structures, the studies have not been quantified precisely but only stopped at general conclusions such as corrosion causes damage [10–12]. In previous studies, Kainuma et al. [13] were conducted accelerated cyclic corrosion exposure tests on 20 uncoated specimens. The specimens consisted of 9mm thick structural steel that was partially embedded in concrete block. The S6-cycle, which was proposed by the Ministry of International Trade and Industry of Japan, was applied. Then, corroded surface data and bearing capacity of corroded steel were also analyzed. The S6-cycle corrosion test was carried out on structural steels for 30, 60, 90, 120 and 150 days and metal coating films for 100, 200 and 300 days by Yoshito Itoh and In-Tae Kim. Then correlation between the S6-cycle test and the field test on uncoated structural steels and metal coated steels can be determined by acceleration coefficients based on flying salt amount. The coefficients were applicable for durability prediction of uncoated, zinc hot-dip galvanized and painted steels [14].

The dynamic loads, it will create direct or potential risks of destroying the structure. The dynamic loads from wind, vibrations of moving vehicles, and earthquakes can influence the behavior of structures. These dynamic loads can cause initial cracking to appear on the surface. Over time, these cracks continuously propagate and develop until the structure is destroyed, which is known as the fatigue behavior of the steel structure. When fatigue occurs, the cracks also become vulnerable points for corrosive substances to penetrate deep inside, leading to the rapid development of cracking under the combined effects of fatigue and corrosion. This can seriously deteriorate the working capacity of the steel structure [15].

Cracks in steel structures often initiate and propagate from the locations of stress concentration. The stress concentrations are the critical structural details to determine the crack initiation and growth life of engineering structures. Despite careful detail-design, practically many structures contain stress concentrations due to corrosion pit. Pit in structural components will create stress concentrations and hence will reduce the mechanical properties. In the study of fatigue behavior, the stress concentration factor K_t is considered the most significant factor showing the impact of fatigue behavior on steel structures, accordingly, corrosion holes combined with fatigue are also of interest to some researchers [16–18]. The stress concentration factor can be totally determined by powerful and accessible numerical analysis such as ABAQUS, ANSYS, SAP etc. [19–22]. Some experts and engineers also studied the relationship between the length of the destructive cracking and fatigue life. Then, the effect of corrosion on the fatigue behavior of corroded steel was also studied [23–26].

In the design of steel structures, stress concentration factor and fatigue issues have been considered and included in the design based on standards. However, to date, the exact design of the working capacity taking into account corrosion has not been standardized. Corrosion prevention can only be done by including safety factors or having a plan for coating and periodic maintenance. This leads to the design of steel structures being very redundant without any way to optimize.

This study focuses on analyzing the fatigue behavior of artificially corroded steel members. The steel structure is created to simulate the working process of steel structures working with concrete in the real environment. Then, the specimens are set up in the CCT600 artificial corrosion machine. This machine creates the corrosion cycle with full parameters such as temperature, humidity, and salt concentration. The corroded specimens after the experiment is put into fatigue testing to determine the effect of corrosion over time on the fatigue behavior of the steel structure. The process of forming and developing cracking leads to a significant decrease in the behavior of the corroded steel structure. The study also proposes a method to determine the stress concentration factor K_t using the finite element method. Based on that the development trend of stress concentration factor K_t can be predicted, as

well as the relationship between the concentrated stress K_t and the corrosion thickness of the corroded steel structure is also proposed.

2. Fatigue test procedures

2.1. Procedure to create corroded specimens

Four (04) types of specimens are named SC-0, SC-20, SC-70 and S as shown in Fig. 1, respectively. Six specimens of each type were arranged into the tester chamber to conduct the corrosion test at 200, 400 and 600 cycles.

Based on the instruction of ASTM D 6899-03 [27], CCT-I cycle was applied to create the corrosion environment. One (01) cyclic corrosion test duration is 8.5 hour, which consisted of 4 h salt mist application, 2 h dry-off, 2 h humidity, and 0.5 h dry-off. CCT-I cycle is controled by Q-Fog CCT600 tester, as shown in Fig. 2.

After the corrosion test, corroded specimens were carefully cleaned through a blasting treatment, as shown in Fig. 3.

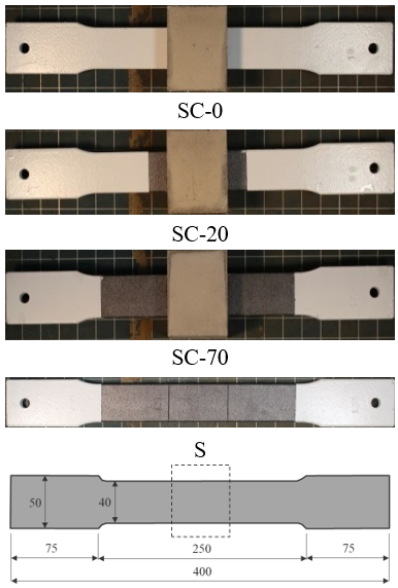

Figure 1. Four types of specimen for corrosion test

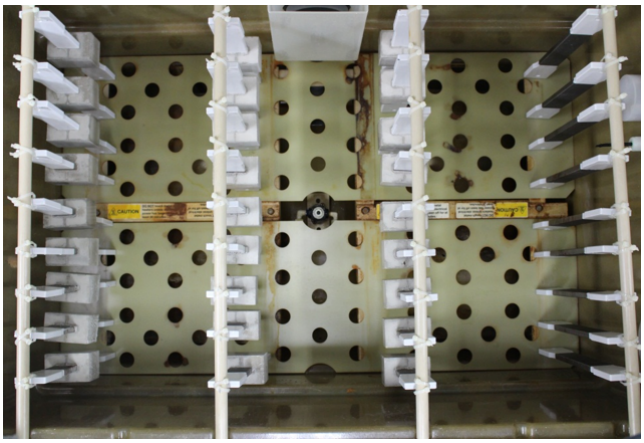

Figure 2. Interior of the instrument chamber and specimen arrangement

Figure 3. Corroded specimens after cleaning

2.2. *Test specimen for fatigue test*

Eighteen (18) corroded specimens of four types of specimen at 200, 400, and 600 cyclic corrosion test and 3 new specimens (un-corroded specimen, were denoted by N) were used to perform fatigue tests, the model of specimen is shown in Fig. 4.

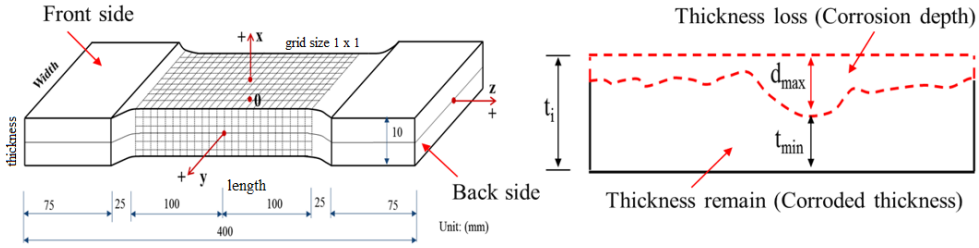

Figure 4. Model of specimens

The summary of characteristics of all specimens shows in Table 1.

Table 1. Summary of the fatigue results

Symbol of specimen	Type of specimen	Number of cycles	Initial thickness (mm)	Width (mm)	t_{min} of avg	Proposed effective $t_{eff} = t_{avg} - S$ (mm)	t_{avg} at failure	Stress range (MPa) of $t_{initial}$	Stress range (MPa) of t_{min} of avg	Stress range (MPa) of t_{eff}	Stress range (MPa) of t_{avg} at failure	Fatigue life (Cycles)	Failure position
200-0-1	0 mm	200	10	40	9.67	9.70		200	207	206		3,000,000	No failure
200-0-2		200	10	40	9.72	9.70		200	206	206		3,000,000	No failure
400-0-1	0 mm	400	10	40	9.53	9.55		200	210	209		3,000,000	No failure
400-0-2		400	10	40	9.61	9.61	9.65	200	208	208	207	2,200,000	Right corner
600-0-1	0 mm	600	10	40	9.02	8.98	8.97	200	222	223	223	2,700,000	Left side
600-0-2		600	10	40	9.17	9.13		200	218	219		830,000	Proceeding
200-20-1	20 mm	200	10	40	8.70	8.73	8.71	200	230	229	230	1,805,000	Left corner
200-20-2		200	10	40	8.72	8.76		200	229	228		3,000,000	No failure
400-20-1	20 mm	400	10	40	8.12	8.07	8.42	200	246	248	237	900,000	Left corner
400-20-2		400	10	40	8.19	8.25	8.89	200	244	242	225	740,000	Left corner
600-20-1	20 mm	600	10	40	7.84	7.67	7.25	200	255	261	276	430,000	Right corner
600-20-2		600	10	40	7.66	7.50	6.90	200	261	267	290	Lost data	Right corner
200-70-1	70 mm	200	10	40	8.55	8.64	8.84	200	234	232	226	1,435,000	Left corner
200-70-1		200	10	40	8.81	8.77	8.87	200	227	228	226	874,700	Left corner
400-70-1	70 mm	400	10	40	7.99	8.02	8.24	200	250	249	243	397,500	Left corner
400-70-2		400	10	40	7.99	8.02	8.26	200	250	249	242	860,000	Right corner
600-70-1	70 mm	600	10	40	7.70	7.46	6.58	200	260	268	304	90,000	Right corner
600-70-2		600	10	40	7.34	7.22	6.35	200	272	277	315	90,000	Right corner
200-S-1	No conc	200	10	40	8.34	8.42	8.47	200	240	238	236	698,500	Left corner
200-S-2		200	10	40	8.49	8.47	8.77	200	236	236	228	1,041,300	Right Side
400-S-1	No conc	400	10	40	7.61	7.62	7.76	200	263	262	258	152,000	Right side
400-S-2		400	10	40	7.79	7.71	7.92	200	257	260	253	297,000	Left side
600-S-1	No conc	600	10	40	6.92	7.06	6.28	200	289	283	319	40,000	Left corner
600-S-2		600	10	40	7.21	7.12	6.58	200	278	281	304	38,000	Right side
N1	New	0	10	40									
N2	New	0	10	40									
N3	New	0	10	40									

2.3. *Fatigue test condition*

According to the KS B0802 (2008) standard [28], fatigue testing conducted in Universal Fatigue Testing Machine (UTM) operating at 8 Hz. The vibration loading (tensile load) amplitude was controlled during the test, which is governed by sine function; the maximal load is −10 kN, and minimum load is −90 kN. Fig. 5 shows the arrangement of fatigue test.

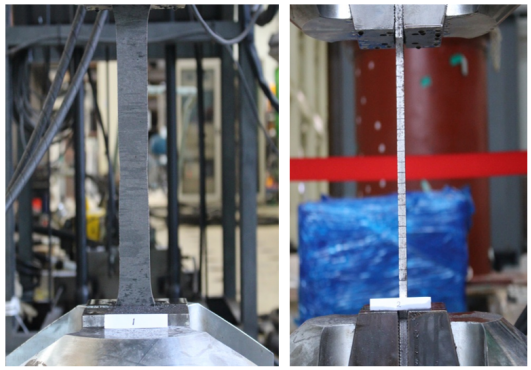

Figure 5. Test setup of fatigue test

3. Results and discussion

3.1. *Influence of corrosion on fatigue behavior*

Table 1 shows the full parameters of the fatigue test and also the experimental results as a summary. Symbol of specimen is given according to the following principle: Number of cycle - Type of specimen - Sequence number. Then, the relationship between corrosion parameters such as thickness, initial cracks, and failure point with the fatigue life (S-N) curve is presented in Fig. 6. The results indicated that corrosion is one of the most important factors, which can create stress concentration on steel structure. Cause corrosion increases the roughness and local holes of the surface. It can be clearly seen that fatigue failure occurs rapidly in the specimen type S, then in the SC-70, SC-20, and SC-0. This result is completely consistent with the similar increase in corrosion rate due to the influence of the coating and the concrete block.

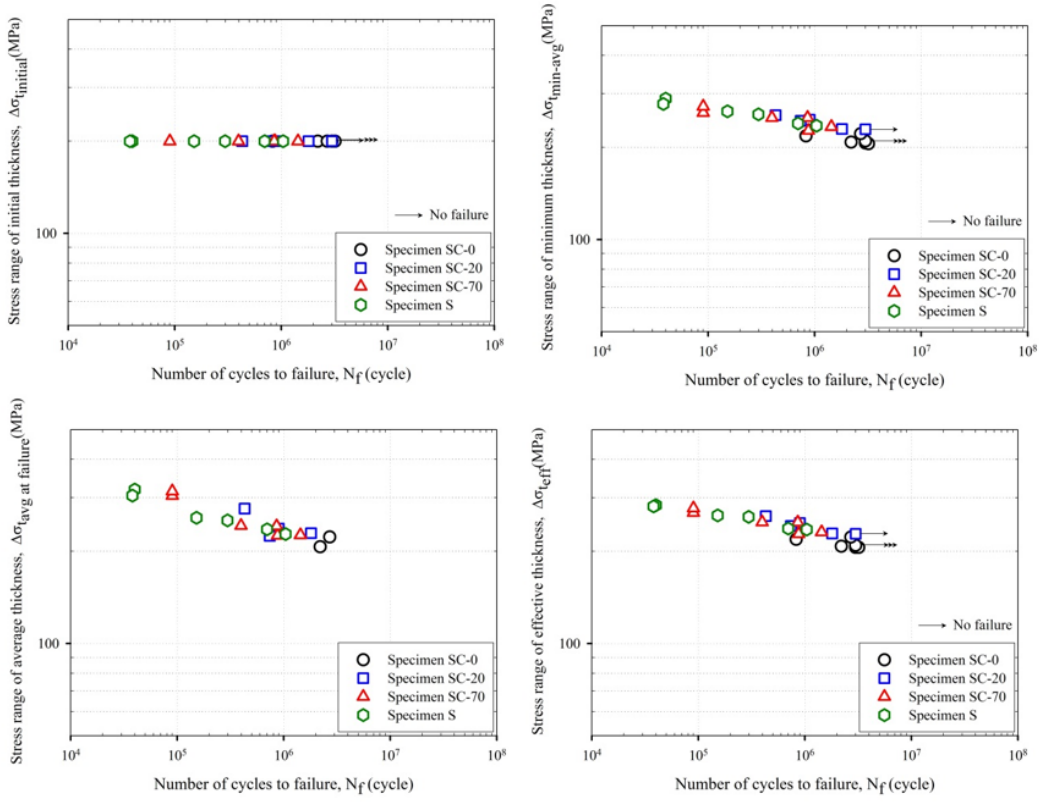

Figure 6. Reduction of fatigue life

3.2. Fatigue Failure mode of corroded steel structure in contact with concrete

In this study, the confidence curve was proposed to design the fatigue life of corroded steel plate in contact with concrete in terms of effective thickness, as shown in Fig. 7. Once established, the fatigue reliability formula provides the designer with properties that can be used with confidence in design. However, this fatigue response curve is only characteristic for the analysis in this study. The factors such as the joint of the steel structure, the connection position between the steel structure and other materials, large steel member, and different environmental conditions have not been analyzed in this study. Therefore, for accurate assessment, additional studies are needed.

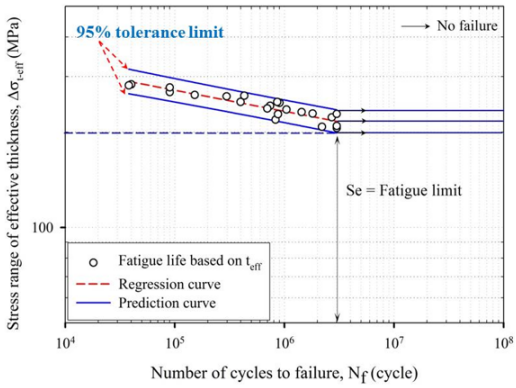

Figure 7. Confident curve

This relatively simple set of procedures produces a reasonable estimate of the tolerance limits for fatigue data used in the damage assessment of steel members exposed to concrete applications. It should be noted that among the problems involved in estimating a fatigue life curve to a certain degree of confidence, the one most likely to make a large difference in the estimated life is the choice of alignment axis. Calculate or logarithm for stress or strain.

4. Analysis of stress concentration factor K_t by finite element method

4.1. Software, element types, mesh construction and material modeling

Advances in computational features and software have brought the finite element method within reach of both academic research and engineers in practice using general-purpose nonlinear finite element analysis packages, with one of the most used nowadays is ANSYS. The program offers a wide range of options regarding element types, material behavior, and numerical solution controls, as well as graphic user interfaces (known as GUIs). In this paper, the structural system modeling is based on the use of this commercial software. The finite element types were chosen in the model of ANSYS 16 [29], as shown in Fig. 8.

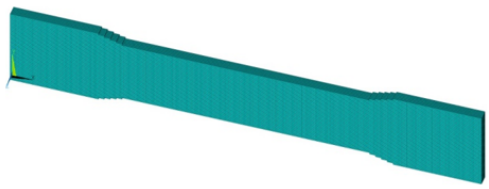

Figure 8. Software, element types and mesh construction

The full model of specimens was built to analyze the nonlinear tensile behavior. Accordingly, the finite element type of steel beam was SOLID95. The element SOLID95 is a higher-order version of the 3-D 8-node solid element SOLID45. It can tolerate irregular shapes without as much loss of accuracy. SOLID95 elements have compatible displacement shapes and are well suited to model curved boundaries. The element is defined by 20 nodes having three degrees of freedom per node: translations in the nodal x, y, and z directions, as shown in Fig. 9. The element may have any spatial orientation. SOLID95 has plasticity,

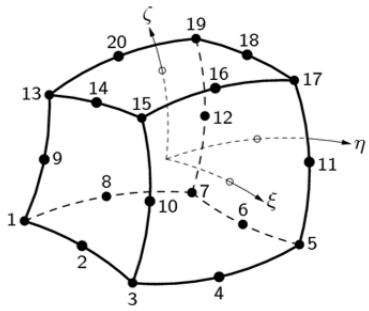

Figure 9. Characteristic of element Solid 95

creep, stress stiffening, large deflection, and large strain capabilities. Various printout options are also available.

In this study, the elastic modulus E = 191 (GPa), Poisson's ratio γ = 0.275 were applied to all analytical models, respectively.

4.2. Boundary condition, application of load and numerical control

The boundary condition was applied to describe exactly with the actual experimental condition. One end of the specimen was fixed in X, Y and Z directions of 70 mm and similarly only the Y and Z direction were fixed in the other end. The applying load was the surface stress of 1 MPa. The FEM conditions for linear analysis shown in Fig. 10.

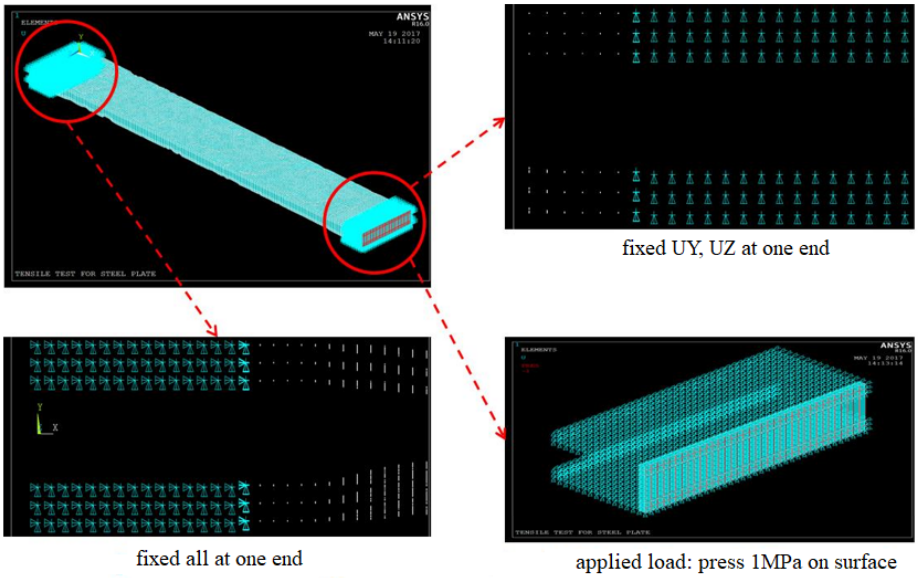

Figure 10. Boundary condition

4.3. FEM results and discussion

a. The effect of the number of layer on stress concentration factor K_t

Cracks in steel structures often initiate and propagate from the locations of stress concentration. The stress concentrations are the critical structural details to determine the crack initiation and growth life of engineering structures. Despite careful detail-design, practically many structures contain stress concentrations due to corrosion pit. Pit in structural components will create stress concentrations and hence will reduce the mechanical properties To evaluate exactly the stress concentration factor K_t of corroded steel plate in contact with concrete. The stress concentration factor K_t was determined by Eq. (1).

$$K_t = \frac{\sigma_{\max}}{\sigma_{nom}} \tag{1}$$

where $\sigma_{\max}$, σ_{nom} are the maximum stress and nominal stress in FEM analysis, under the applying load of 1 MPa on all the surface, the nominal stress was always 1 MPa.

In this study, we recognized that stress concentration factor K_t is affected by the mesh size, and the number of layer in FEM model. Before the analysis of stress concentration factor K_t on the corroded steel plate in contact with concrete, the effect of the number of layer on stress concentration factor K_t was assessed carefully by 2D and 3D FEM model as shown in Fig. 11, in two cases:

- The effect from 1 to 9 layers were divided from up to down, as shown in Fig. 12;
- The effect from 1 to 9 layers were divided from both side, as shown in Fig. 13.

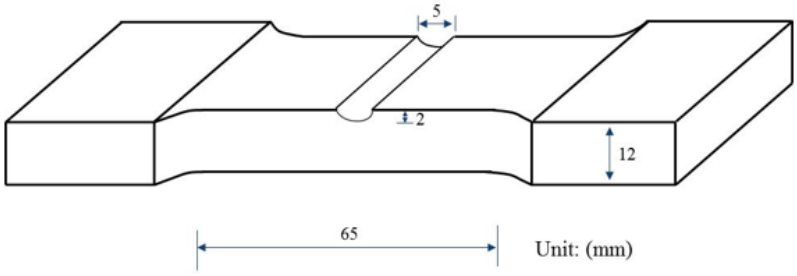

Figure 11. Model for analysis of the effect of the number of layer

Case 1: Dividing the layer from up to down

After analysis, the relationship value of K_t and number of layer shows in Fig. 10. Accordingly, the K_t was increased as the number of layer increased, and then K_t reached the consistence value at layer 4th. After that, the value of K_t was almost constant, so in the analysis of stress concentration factor K_t, the FEM model should be divided at least 4 layers.

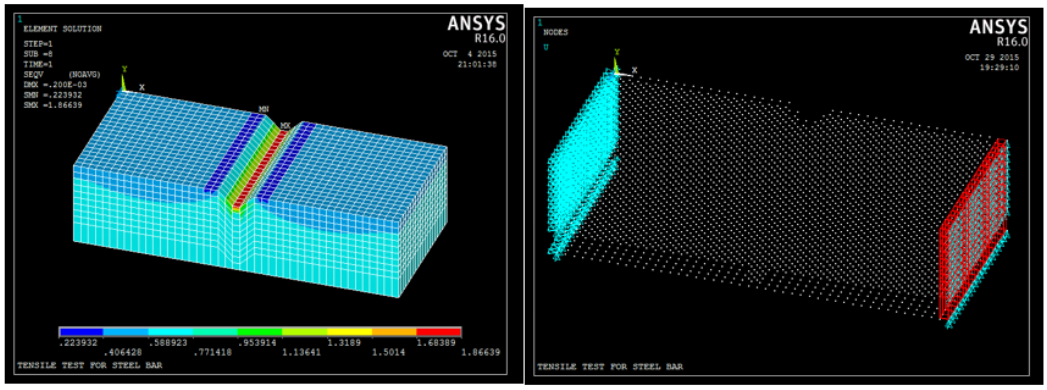

Figure 12. Model and boundary condition of in 3D

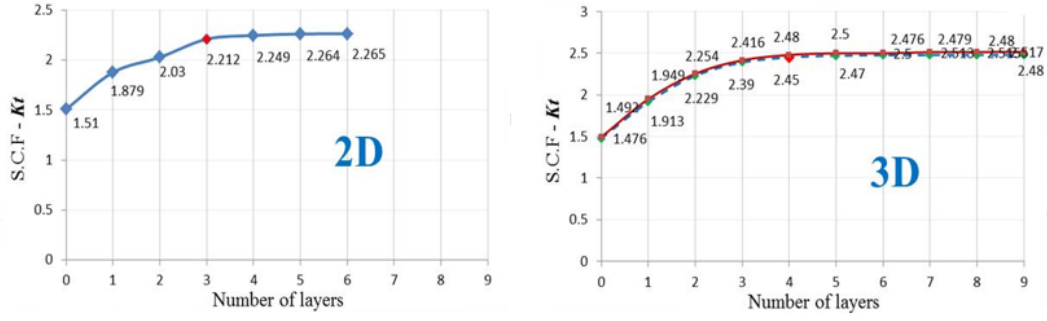

Figure 13. Relationship of Stress concentration K_t and number of layer

Case 2: Dividing the layer from the both side

After analysis, the relationship value of K_t and number of layer shows in Fig. 14. Accordingly, the K_t was increased as the number of layer increased, and then K_t reached the consistence value at

layer 2nd for the both side. After that, the value of K_t was almost constant, so in the analysis of stress concentration factor K_t, the FEM model should be divided at least 2 layers at the both side, as shows in Fig. 15.

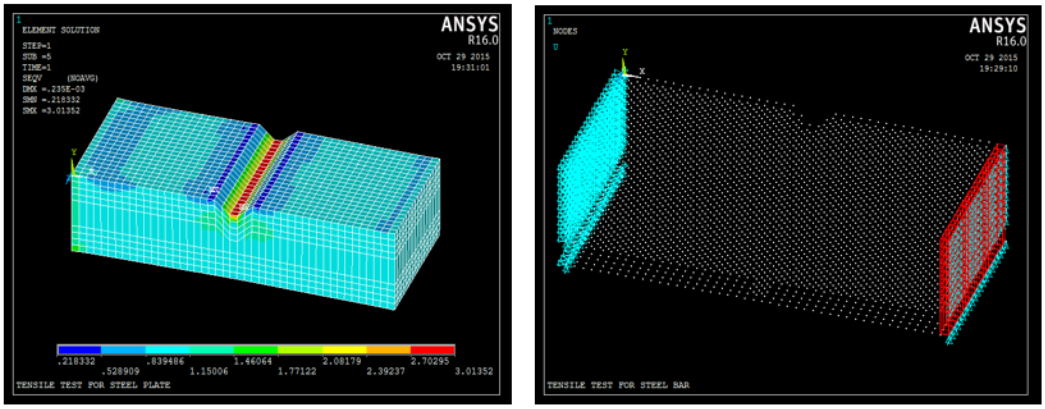

Figure 14. Model and boundary condition of in 3D

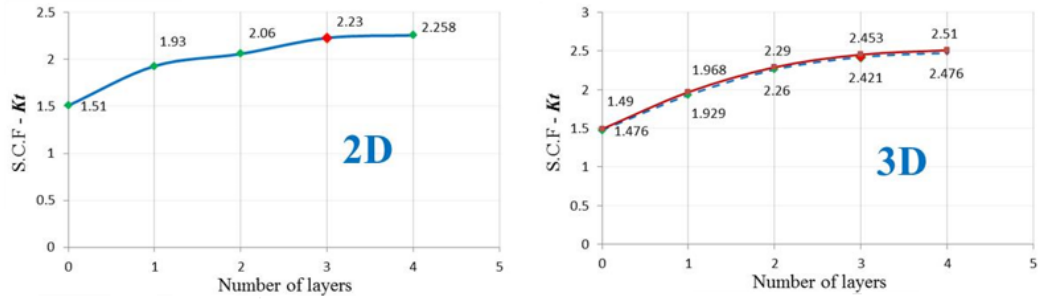

Figure 15. Relationship of Stress concentration K_t and number of layer

b. Estimation of fatigue life by FEM analysis

Since the analysis of the present investigation is entirely based on finite element modeling and its results, the verification of the developed finite element models is considered very essential. Based on the achievement of FEM analysis, the K_t at the failure position was determined by FEM. Also, the detail of failure shape, initial crack and crack propagation of all specimens shown in Fig. 16. It can be seen that crack initiation areas are all around the specimen surface due to corrosion pits. A typical fracture of each fatigue specimen consists of fatigue crack initiation zone, fatigue crack growth zone, and instantaneous fracture zone were show in Fig. 16. In general, there was only one or two critical crack in each specimen, although several cracks were observed to initiate within the corrosion sections. We have evaluated the critical cracks of all corroded specimens based on fracture images analysis.

The relationship between stress concentration factor K_t presents in Fig. 17. Fig. 17(a) shows the relationship between minimum of average thickness $t_{\min-avg}$ and stress concentration factor K_t. Fig. 17(b) shows the relationship between effective thickness t_{eff} and K_t. The results show that t_{eff} has a higher agreement in relation to K_t. Therefore, when determining K_t, the t_{eff} value is recommended to be included in the calculation.

The results proofed that stress concentration factor K_t is inverse ratio with residual measured thickness. The K_t of corroded steel plate in contact with concrete can be totally estimated by residual

measured thickness using t_{eff}, as shown in Eq. (2) and Eq. (3).

$$K_t = 0.6154 + 21.75e^{-0.3894t_{\min-avg}}, \quad R^2 = 0.915 \tag{2}$$

$$K_t = 1.0357 + 157.04e^{-0.7128t_{eff}}, \quad R^2 = 0.933 \tag{3}$$

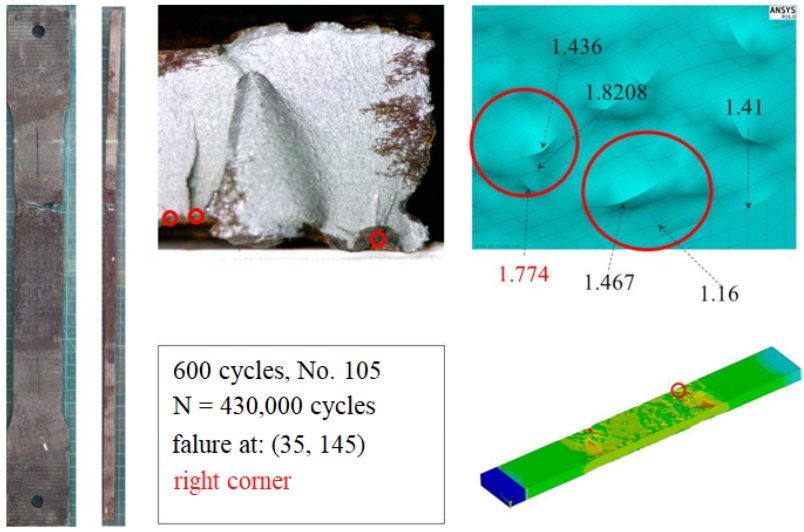

Figure 16. Failure mode and stress concentration factor at failure point of specimens

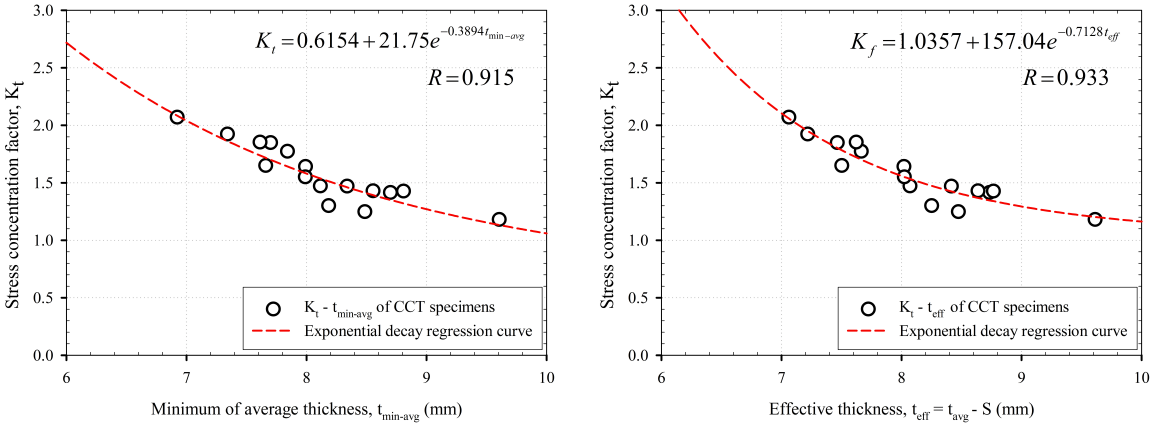

(a) Minimum of average thickness

(b) Effective thickness

Figure 17. Estimation of stress concentration factor by measured thickness

5. Conclusions

21 specimens of four types of steel plates in contact with concrete were chosen for fatigue testing. The study quantitatively evaluated the fatigue life of a corroded steel plate in contact with concrete by analyzing the S-N curve, crack characteristics, and stress concentration coefficient based on the remaining thickness. The following conclusions can be drawn from this study:

- Corrosion will cause a significant decrease in fatigue life, with the corrosion increased the fatigue life decreased.

- The reduction of fatigue life S-N curves of specimen type S was reduced faster than the other and next was the specimen type SC-70, SC-20 and SC-0, respectively.

- The stress concentration factor K_t will be affected by number of layer in FEM model. The FEM model for analysis of stress concentration factor K_t should be divided by at least 4 layers at one side or 2 layers at the both side.

- In each sample, only one or two significant cracks were found, although some cracks were seen to start in the corroded areas. The findings show that the stress concentration coefficient (K_t) is inversely related to the remaining measured thickness. The K_t of a corroded steel plate in contact with concrete can be determined solely by the remaining measured thickness.

References

[1] Reza Khedmati, M., Mahdi Roshanali, M., Mohammad Esmaeil Nouri, Z. H. (2011). Strength of steel plates with both-sides randomly distributed with corrosion wastage under uniaxial compression. *Thin-Walled Structures*, 49(2):325–342.

[2] Sankaran, K. K., Perez, R., Jata, K. V. (2001). Effects of pitting corrosion on the fatigue behavior of aluminum alloy 7075-T6: modeling and experimental studies. *Materials Science and Engineering: A*, 297(1–2):223–229.

[3] Zahrai, S. M. (2003). Cyclic Strength and Ductility of Rusted Steel Members. *Asian Journal Of Civil Engineering (Building And Housing)*, 4:135–148.

[4] Rusk, D., Hoppe, W. (2009). Fatigue life prediction of corrosion-damaged high-strength steel using an equivalent stress riser (ESR) model Part I: Test development and results. *International Journal of Fatigue*, 31(10):1454–1463.

[5] Rusk, D., Hoppe, W., Braisted, W., Powar, N. (2009). Fatigue life prediction of corrosion-damaged high-strength steel using an equivalent stress riser (ESR) model. Part II: Model development and results. *International Journal of Fatigue*, 31(10):1464–1475.

[6] Beretta, S., Carboni, M., Fiore, G., Lo Conte, A. (2010). Corrosion–fatigue of A1N railway axle steel exposed to rainwater. *International Journal of Fatigue*, 32(6):952–961.

[7] Palin-Luc, T., Pérez-Mora, R., Bathias, C., Domínguez, G., Paris, P. C., Arana, J. L. (2010). Fatigue crack initiation and growth on a steel in the very high cycle regime with sea water corrosion. *Engineering Fracture Mechanics*, 77(11):1953–1962.

[8] Schönbauer, B. M., Stanzl-Tschegg, S. E., Perlega, A., Salzman, R. N., Rieger, N. F., Zhou, S., Turnbull, A., Gandy, D. (2014). Fatigue life estimation of pitted 12% Cr steam turbine blade steel in different environments and at different stress ratios. *International Journal of Fatigue*, 65:33–43.

[9] Gruenberg, K. M., Craig, B. A., Hillberry, B. M., Bucci, R. J., Hinkle, A. J. (2004). Predicting fatigue life of pre-corroded 2024-T3 aluminum from breaking load tests. *International Journal of Fatigue*, 26(6): 615–627.

[10] hua Xu, S., Qiu, B. (2013). Experimental study on fatigue behavior of corroded steel. *Materials Science and Engineering: A*, 584:163–169.

[11] van der Walde, K., Hillberry, B. (2007). Initiation and shape development of corrosion-nucleated fatigue cracking. *International Journal of Fatigue*, 29(7):1269–1281.

[12] van der Walde, K., Hillberry, B. M. (2008). Characterization of pitting damage and prediction of remaining fatigue life. *International Journal of Fatigue*, 30(1):106–118.

[13] Kainuma, S., Hosomi, N. (2008). Fatigue life evaluation of corroded structural steel members in boundary with concrete. *International Journal of Fracture*, 157(1–2):149–158.

[14] Itoh, Y., Kim, I. (2006). Accelerated cyclic corrosion testing of structural steels and its application to assess steel bridge coatings. *Anti-Corrosion Methods and Materials*, 53(6):374–381.

[15] Codaro, E., Nakazato, R., Horovistiz, A., Ribeiro, L., Ribeiro, R., Hein, L. (2002). An image processing method for morphology characterization and pitting corrosion evaluation. *Materials Science and Engineering: A*, 334(1–2):298–306.

[16] Chuan, Z., Yanhui, C., Weixing, Y. (2014). The use of fractal dimensions in the prediction of residual fatigue life of pre-corroded aluminum alloy specimens. *International Journal of Fatigue*, 59:282–291.

[17] Carpinteri, A., Spagnoli, A., Vantadori, S. (2009). Size effect in S–N curves: A fractal approach to finite-life fatigue strength. *International Journal of Fatigue*, 31(5):927–933.
[18] Biancolini, M. E., Brutti, C., Paparo, G., Zanini, A. (2006). Fatigue cracks nucleation on steel, acoustic emission and fractal analysis. *International Journal of Fatigue*, 28(12):1820–1825.
[19] Kainuma, S., Jeong, Y.-S., Ahn, J.-H. (2014). Investigation on the stress concentration effect at the corroded surface achieved by atmospheric exposure test. *Materials Science and Engineering: A*, 602: 89–97.
[20] Luna, V. M., Kim, I.-T., Jeong, Y.-S. (2024). Stress concentration factor estimation for corroded steel plates using the surface gradient method. *Engineering Failure Analysis*, 163(Part B).
[21] She, C., Guo, W. (2007). Three-dimensional stress concentrations at elliptic holes in elastic isotropic plates subjected to tensile stress. *International Journal of Fatigue*, 29(2):330–335.
[22] Arola, D. D., Williams, C. E. (2002). Estimating the fatigue stress concentration factor of machined surfaces. *International Journal of Fatigue*, 24(9):923–930.
[23] Garbatov, Y., Guedes Soares, C., Parunov, J. (2014). Fatigue strength experiments of corroded small scale steel specimens. *International Journal of Fatigue*, 59:137–144.
[24] hua Xu, S., de Wang, Y. (2015). Estimating the effects of corrosion pits on the fatigue life of steel plate based on the 3D profile. *International Journal of Fatigue*, 72:27–41.
[25] Cerit, M., Genel, K., Eksi, S. (2009). Numerical investigation on stress concentration of corrosion pit. *Engineering Failure Analysis*, 16(7):2467–2472.
[26] Cerit, M. (2013). Numerical investigation on torsional stress concentration factor at the semi elliptical corrosion pit. *Corrosion Science*, 67:225–232.
[27] ASTM Designation: D6899-03. 2003 (2003). *Standard Guide for Laboratory Cyclic Corrosion Testing of Automotive Painted Steel*.
[28] KS B 0802:2003 (2003). *Method of Tensile Test for Metallic Materials*. Korean Agency for Technology and Standards.
[29] Ansys (2013). *Mechnical APDL Material Reference, Release 16*. Ansys Inc.